Spectroscopic studies on copper(II) complexes of chiral cyclens: [CuN_4Cl] chromophores varying from square pyramidal to trigonal bipyramidal stereochemistry

Nagao Azuma*
Department of Chemistry, Faculty of General Education, Ehime University, Matsuyama 790 (Japan)

Yuji Kohno, Fujito Nemoto, Yuji Kajikawa and Kazuhiko Ishizu*
Department of Chemistry, Faculty of Science, Ehime University, Matsuyama 790 (Japan)

Takashi Takakuwa
Application Laboratory, JASCO Corporation, Hachiohji 921 (Japan)

Sei Tsuboyama*, Kaoru Tsuboyama, Kimiko Kobayashi and Tosio Sakurai
The Institute of Physical and Chemical Research (RIKEN), Wako, Saitama 351-01 (Japan)

(Received May 12, 1993; revised July 30, 1993)

Abstract

A series of five copper(II) complexes with four geometrically isomeric ligands of 1,4,7,10-tetrabenzyl-2,5,8,11-tetraethyl-1,4,7,10-tetraazacyclododecane and with (2*R*,5*R*,8*R*,11*R*)-2,5,8,11-tetraethyl-1,4,7,10-tetraazacyclododecane has been investigated by means of ESR, CD and MCD in solution. X-ray studies reported separately had shown that the [CuN_4Cl] chromophores were distorted to varying extents from square pyramidal to trigonal bipyramidal geometry. The stability and rigidity of the molecular structure have enabled us to carry out a complementary study of the crystalline state and solution chemistry The ground state Kramers doublets varied from $3d_{x^2-y^2}$ to $3d_{z^2}$ type with increasing distortion around the copper ion. The orbital sequence of the $3d^1$ positive hole, $d_{x^2-y^2} < d_{z^2} < d_{yz,xz} < d_{xy}$, has been obtained for the C_{4v} complexes The $3d_{xy}$ orbital is also the highest in energy for the complex with the $3d_{z^2}$ type ground state doublet. This complex exhibited superhyperfine splitting in the g_z region due to the chlorine nucleus, which implies the principal z axis of the g tensor is along the Cu–Cl bond. The sign of the copper hyperfine tensors was determined by means of Swalen's treatment The changing values of the orbital coefficients decreasing for the $3d_{x^2-y^2}$ and increasing for the $3d_{z^2}$, $3d_{xz}$ and $3d_{yz}$ in the ground state doublets have been attributed to concomitant elongation of the in-plane Cu–N bond and reduction of the out-of-plane Cu–Cl bond length with the increasing distortion around the copper ions.

Key words: Copper complexes; Macrocyclic ligand complexes

Introduction

As shown in Fig. 1, the chiral macrocyclic ligand, 1,4,7,10-tetrabenzyl-2,5,8,11-tetraethyl-1,4,7,10-tetraazacyclododecane (tbte) can be resolved into four geometrical isomers and the former two in turn into enantiomeric pairs [1]. The molecular structures of the four geometrical and two optically active isomers have been determined [2]. Further, the non-N-substituted optically active cyclen, (2*R*,5*R*,8*R*,11*R*)-2,5,8,11-tetraethyl-1,4,7,10-tetraazacyclododecane (te_R), was also prepared [3] and characterized [4]. These tetradentate cyclens react with copper chloride to yield the copper(II) complexes named as **A** ($\mathbf{A}_R$ and $\mathbf{A}_S$), **B**, **C**, **D** and te**A** ($te\mathbf{A}_R$ and $te\mathbf{A}_S$) and shown in Fig. 2**.

All the complexes are penta-coordinate, of the type [CuCl(chiral cyclen)]Cl. The chloride ion is coordinated at the apex of a pyramid. The counter-anion is at the

*Authors to whom correspondence should be addressed

Although the data of **A and te**A** were actually obtained by using the respective optically active complexes, the designations are applied for convenience. In fact, **A**, $\mathbf{A}_R$ and $\mathbf{A}_S$ revealed identical spectra, except for the CD of $\mathbf{A}_S$, which showed a spectrum exactly enantiomeric to that of $\mathbf{A}_R$.

SSDI 0020-1693(93)03677-3

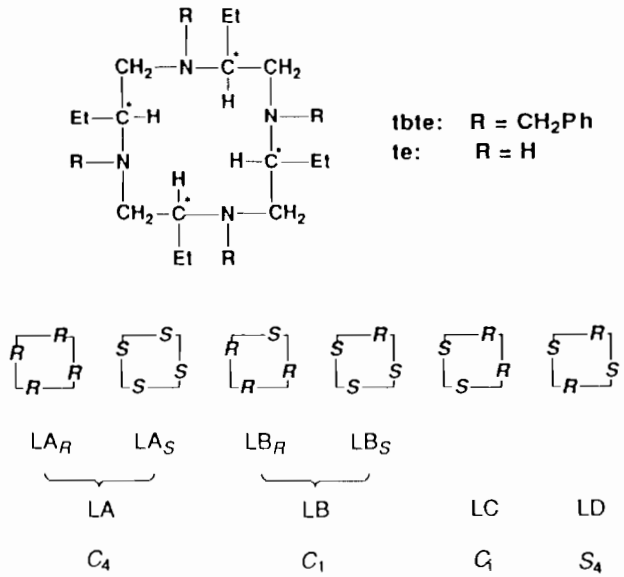

Fig 1 Configuration, geometrical isomers and symmetry of the chiral cyclen ligands

opposite side of the apical chloride ion and located far from the copper ion in the crystal (>4.48 Å). The stereochemistry around the copper ion varies from square pyramidal to trigonal bipyramidal, depending on the configuration of the ligand. The distortion from the square pyramid towards the trigonal bipyramid can be expressed along the Berry coordinate [5a]. The displacement percentage (tbp%) is increased in the order of te**A**=**A**<**C**<**B**≪**D** (see Table 1) [6]. Another angular-structure parameter for trigonality, τ [5b], indicates the same order. For certain compounds, a trigonal bipyramidal geometry in solution is rapidly interconverted to another one via a square pyramidal configuration [7]. Stereochemical fluxionality is a ubiquitous feature of penta-coordination [8]. Ray *et al.* [9] reported crystal structures and electronic reflectance spectra of cation distortion isomers with $[CuN_5]$ chromophores, making relation to the 'plasticity effect'. In such a case, the individual stereochemistries in solution must be considerably different from those in their crystal, because weak interactions, such as van der Waals and hydrogen bonding forces control the stereochemistry. Thus the $3d_{z^2}$ ground state established for the crystal of $[Cu(bipy)_2(thiourea)](ClO_4)_2$ shifted to a $3d_{x^2-y^2}$ ground state in an *N,N*-dimethylformamide glass [10]. Therefore, the complementary studies of the crystalline state and solution chemistry of such complexes should be difficult except under special circumstances. In the present work, these are achieved with the particular ligand construction mentioned below.

Since the structure of the ion site of penta-coordinate copper is inherently fluxional, stereochemical variation due to the requirements of chelating ligands can often be found in individual complexes. The present chiral cyclens have a small size N_4 cavity and bulky substituents, and the copper ion is above the plane of the four nitrogen atoms, so the N_4 donor set combines with the copper ion loosely in-plane, as seen in Fig. 2 [11]. A similar stereochemistry to that of **A** can also be seen in [CuCl(1,4,7,10-tetrabenzylcyclen)]NO_3 [12a]. Therefore, it is also noted that the present work is a study for penta-coordination of the copper(II) ion bound loosely in-plane.

The present cyclens have four chiral centers due to the ethyl groups; they have four N-benzyl groups adjacent to every chiral center. The presence of many such substituents results in a rigid molecular structure even for the penta-coordinate copper. Complex **D** with a $3d_{z^2}$ type ground state Kramers doublet exhibits a reversed relation between the axial and equatorial bond lengths to that expected for the regular d^9-copper trigonal bipyramid. It has been actually implied by spectral evidence that this tight geometry in the crystal remains unchanged in both mobile and low temperature glass media.

The basal Cu–N bond lengths in the present complexes are in a rather wide range, from 2.03 to 2.13 Å as shown in Table 1. In contrast, those for most $[CuN_4X]$ square pyramids with acyclic ligands are in a very narrow range, from 1.98 to 2.03 Å, and the copper displacement from the N-basal plane is less than 0.3 Å [13]. Interestingly, the copper displacement of the present complexes reaches between 0.53 and 0.63 Å with reduction of the Cu–Cl bond distance (2.430–2.354 Å). These Cu–Cl bond lengths are closer to the in-plane bond lengths of ordinary copper(II) complexes (2.25–2.35 Å) than to the out-of-plane ones (2.73–3.20 Å) [14]. This indicates the following characteristics of the present complexes. The cyclens with the small N_4 cavity are so rigid that the lobes of lone pair orbitals on the nitrogen atoms can turn their direction neither down nor up. The in-plane Cu–N bond lengths are accordingly elongated, which causes concomitant reduction of the Cu–Cl bond distance. Thus we can regard the complexes as axially compressed square pyramidal copper(II) ones. Nevertheless, we sometimes use the terms of trigonal bipyramidal distortion, because this terminology is in use.

Electron spin resonance (ESR), visible and near-IR absorption (AB), circular dichroism (CD) and magnetic circular dichroism (MCD) were applied to their mobile and glassy solutions. The energies of AB maxima were observed in the order of te**A**>**A**>**C**>**B**>**D**. The same order appeared in the $|A_z|$ values, the absolute z component of the copper hyperfine coupling tensor A. The reverse sequence to $|A_z|$ has been observed in g_z values, the z component of the g tensor.

Crystal-field calculations are not well suited for the treatment of covalently binding coordination such as

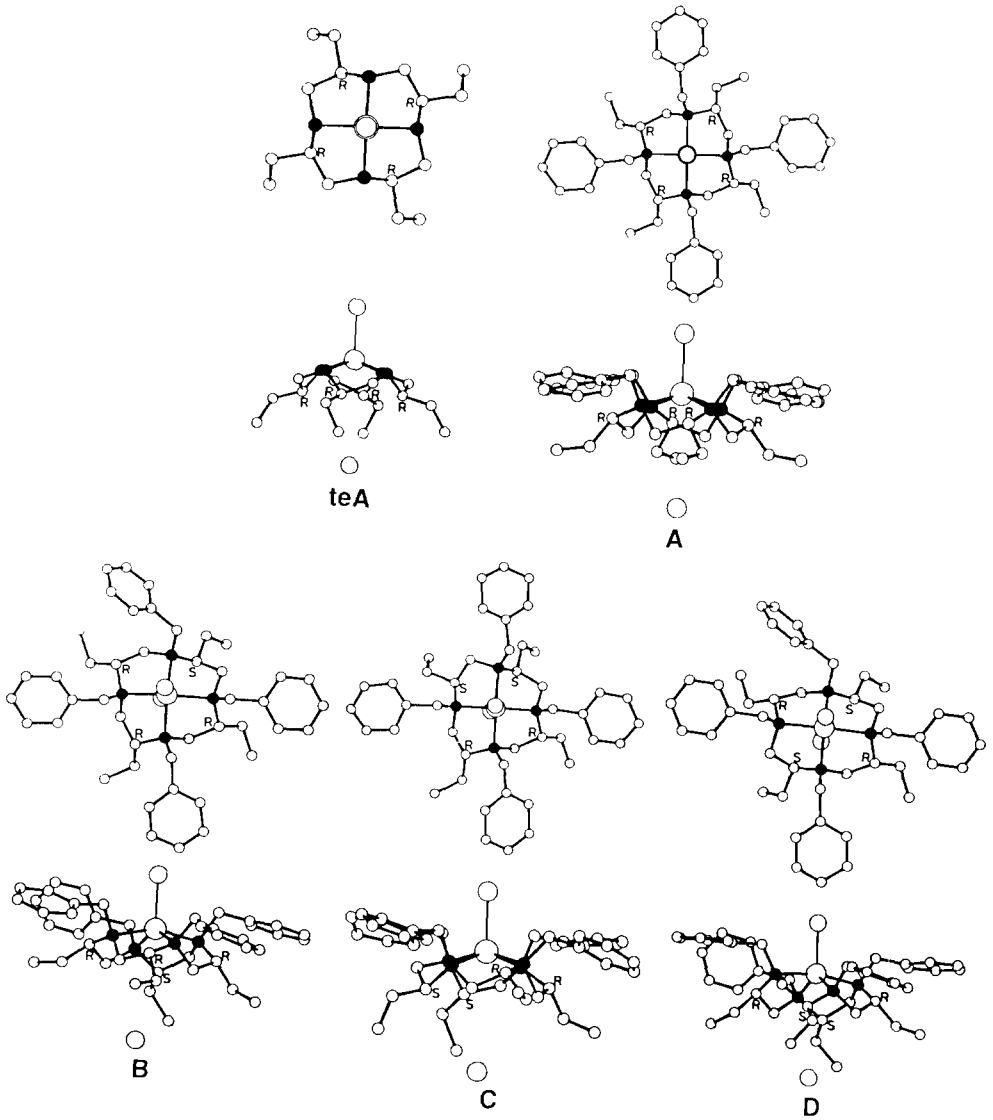

Fig. 2. Plane and side views of the molecular structures of the copper(II) complexes determined by means of X-ray diffraction [11]

these Cu–N bonds. Nevertheless, we have adopted these calculations in order to obtain an auxiliary means for the complementary studies of the crystalline state and solution chemistry. The treatment of Swalen *et al.* [15] of the ground state Kramers doublet has been successfully applied to this series of complexes. The results agree very well with the stereochemistries in the crystals of the respective complexes.

Experimental

Preparation of the complexes

The complexes were prepared by the procedure reported elsewhere [11a]. All the complexes were identified by magnetic susceptibility, elemental analysis and field desorption mass spectral data. The zinc(II) analogue of **D** was prepared by heating an equimolar mixture of zinc chloride and the corresponding ligand (1 mmol) in absolute ethanol (25 ml). Crystals of the zinc complex were obtained by recrystallization from a 1:1 mixed solvent of acetonitrile and ethyl acetate. The mixture of a 0.1 molar ratio of **D** and the zinc analogue was dissolved in the same solvent, and the copper-doped crystals were isolated. The crystal data of the zinc complex are as follows: triclinic, $P\bar{1}$, $a = 13.605(7)$, $b = 15.199(5)$, $c = 11.518(6)$ Å, $\alpha = 109.43(3)$, $\beta = 98.05(4)$, $\gamma = 86.94(4)°$, $V = 2224(2)$ Å^3, $Z = 2$. Although the anion part that contains zinc and chloride ions was not well defined owing to the disorder, the molecular geometry of the Zn–cyclen complex was clearly found to be quite similar to that of **D**: $R = 0.13$.

TABLE 1 Molecular dimensions of the copper(II) complexes of the chiral cyclens in the crystal

Complex	teA [11a]	A [11a]	C [11c]	B [11d]	D [11b]
Trigonal bipyramidal percentage (tbp%)[a]	0	0	20	30	70
Angular trigonality parameter (τ)[b]	0 010	0 027	0 095	0 328	0 670
Ligand field symmetry approximated[c]	C_{4v}	C_{4v}	C_{4v}	C_{2v}	C_{2v}
Displacement of Cu(II) from N-basal plane (Å)	0 546	0.541	0.528	0 526	0 628
Cu–N bond lengths (Å) average of *trans*-pair A	2.027	2.049	2.07	2.08	2 066
average of *trans*-pair B	2.032	2.071	2.09	2.10	2 130
N–Cu–N bond angle (°) α for *trans*-pair A	148 4	150.4	153 6	138.0	124.2
β for *trans*-pair B	149 0	148.8	147 9	157.7	164.4
Cu–Cl bond length (Å)	2 430	2 400	2 381	2 371	2 354
Cl–Cu–N bond angle θ (°) average of *trans*-pair A	105.8	104 8	103 2	111 0	117.9
average of *trans*-pair B	105 5	105 6	106 1	101.1	97.9
$\Delta\theta$ (°)	0.3	0.8	2.9	9 9	20.0

[a]According to representation of Holmes and Deiters [5a]. [b]The definition $\tau=(\alpha-\beta)/60$ [5b] Therefore, the τ value is very close to $\Delta\theta/30$, where $\Delta\theta$ is the same as that in the botton row of this Table. [c]The exact symmetry in the crystal for teA and A is C_{2v} and the individual bond lengths are therefore equal to the averages Those for the rest are C_1, but can be approximated as the C_{4v} and C_{2v} symmetry designated.

Physical measurements

ESR measurements were carried out in a toluene (5–10%)–chloroform solution but for teA ethanol was used because of its poor solubility in the former solvent. ESR spectra were recorded in glassy solution at 77 K and in mobile solution at room temperature on a JES-ME-3X spectrometer operating with 100 kHz field modulation. The magnetic field strength was calibrated from the hyperfine splitting of the manganese(II) ion (8.69 mT) in powdered magnesium oxide. The g values were determined by taking the Li–TCNQ radical salt to be $g=2.0025$. In order to compare the ESR parameters in the glassy solution with those in the crystal, single crystal ESR measurements were carried out for **D** doped in the single crystal of the zinc(II) analogue at room temperature. The procedure for the experiment and analysis of the data was similar to that described elsewhere [16]. The ESR parameters obtained for **D** in the crystal are as follows: $g_z=2.008$, $g_x=2.245$, $g_y=2.156$; $|A_z|=43\times10^{-4}$, $|A_x|=122\times10^{-4}$, $|A_y|=71\times10^{-4}$ cm^{-1}. The estimated standard deviations for the g and A components are 0.007 and 5×10^{-4} cm^{-1}, respectively. The ESR parameters agree with those obtained from the glassy solution within the limit of three times the standard deviations. The orientational relation between the principal and molecular coordinate system is unspecified, owing to the irregular shape and poor X-ray scattering quality of the crystal used in the ESR measurement.

The optical spectra were measured in chloroform solution, except for teA when methanol was used, at room temperature. The AB spectra were taken with a Hitachi 330 spectrophotometer. The MCD at 1.08 T and CD spectra were recorded on JASCO J-20A, J-200 and J-500 spectropolarimeters.

Results and discussion

Calculation

For the sake of a prospective insight, a simplistic crystal-field calculation is applied to the $3d^1$ positive hole. A C_{4v} square pyramid can be changed to a D_{3h} trigonal bipyramid through a pathway maintaining a C_{2v} distorted square pyramid [7, 8a]. **A** and teA can be approximated as C_{4v} symmetry with safety, **C** can be regarded as C_{4v} rather than C_{2v}, and **B** and **D** as C_{2v} from the crystallographic evidence

In order to see the effects of the copper displacement from the N-basal plane of the C_{4v} square pyramid, the energy levels are calculated as functions of θ ($=\theta_x=\theta_y$) in Fig 3 for a given R (1.988 Å was taken as the radius of the N_4 cavity). The parameters in this Figure are formulated as:

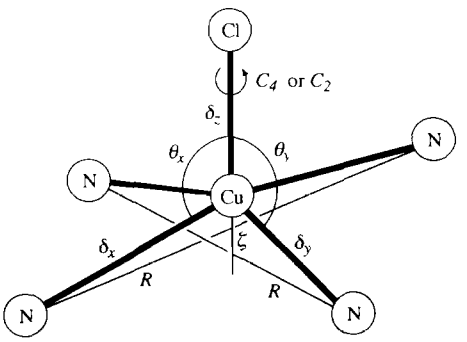

Fig 3. Distortion diagram of the [CuN_4Cl] pyramid. C_4 or C_2 means four- or two-fold axis along the z axis. R stands for the radius of the N_4 cavity The Cu–N bond distances along the x and y direction are defined by δ_x and δ_y; δ_z is the Cu–Cl bond distance The extent of the copper displacement from the N-basal plane is measured by ζ

$$\delta_x = \delta_y = R/\sin\theta \quad (1a)$$

$$\delta_z = \text{constant (2.400 Å)} \quad (1b)$$

$$\zeta = R\tan(\theta - 90) \quad (1c)$$

The crystal-field parameters were estimated from the MCD spectrum for **A**: $\Delta E_{x^2-y^2,\,yz,\,xz} = 13.4$ kcm^{-1} and $\Delta E_{x^2-y^2,\,xy} = 15.6$ kcm^{-1} where ΔE is the energy difference between the designated 3d type levels. This implies that the ground state is the common $3d_{x^2-y^2}$ type and $d_{xy} > d_{yz,\,xz}$ in energy. The calculated energy levels for the $3d^1$ positive hole are shown in Fig. 4. The general features of this level structure are similar to those for a third series transition metal calculated by Rossi and Hoffmann [8a], who treated a C_{4v} square pyramid by means of the molecular orbital theory.

The $3d_{x^2-y^2}$ type ground state Kramers doublet wave functions are composed of $3d_{x^2-y^2}$, $3d_{xy}$, $3d_{yz}$ and $3d_{xz}$ orbitals (refer to eqns. (6)); the latter three are admixed with the former by the spin–orbit coupling $\lambda \boldsymbol{L}\cdot\boldsymbol{S}$. The $\boldsymbol{g}$ tensor components were obtained as functions of θ based on the spin Hamiltonian of the form $\beta\boldsymbol{L}\cdot\boldsymbol{H} + g_e\beta\boldsymbol{S}\cdot\boldsymbol{H}$, for example:

$$g_z = g_e - 2g_e(d^2 + e^2) + 8bc + 4de \quad (2)$$

where g_e is the free electron g value. The coefficients, c, d and e, for the $3d_{xy}$, $3d_{yz}$ and $3d_{xz}$ orbitals are:

$$c = \lambda/\Delta E_{x^2-y^2,\,xy} \quad (3a)$$

$$d = 0.5\lambda/\Delta E_{x^2-y^2,\,yz} \quad (3b)$$

$$e = -0.5\lambda/\Delta E_{x^2-y^2,\,xz} \quad (3c)$$

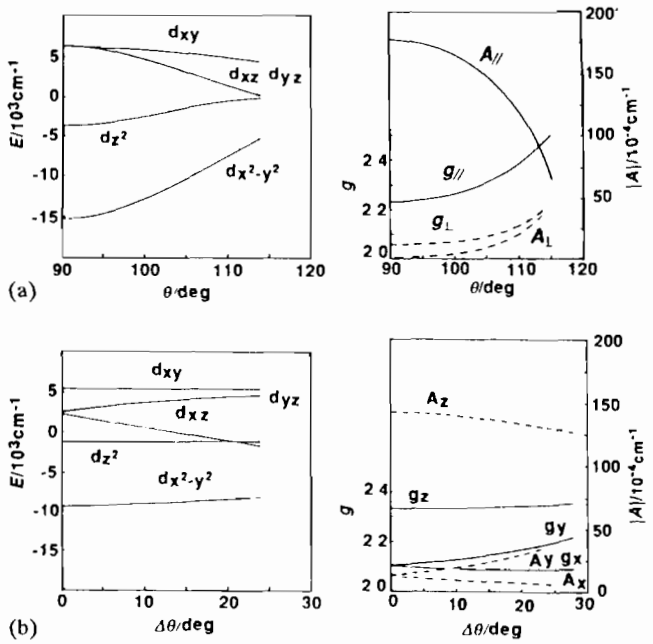

Fig 4 Energy levels and ESR parameters of a 3d positive hole calculated for (a) the C_{4v} and (b) the C_{2v} ligand field symmetry.

where ΔEs are functions of θ. The components of the copper hyperfine coupling tensor were calculated after Abragam and Pryce [17]. The calculated $g_z = g_\parallel$, $g_x = g_y = g_\perp$, $A_\parallel$ and $A_\perp$ are shown in Fig. 4.

In order to speculate how the spectroscopic parameters are affected by the C_{2v} distortion about the Cu–Cl axis, the crystal field Hamiltonian for C_{2v} symmetry was expanded into two terms:

$$V_c = V_{4v} + V_{2v} \quad (4)$$

The second term was treated as a perturbation acting on the first term. The calculation was made by using variable $\Delta\theta(=\theta_x - \theta_y)$ and constant $(\theta_x + \theta_y)/2$. The following constants were used tentatively: $\delta_x = 2.129$ Å, $\delta_y = 2.066$ Å, $(\theta_x + \theta_y)/2 = 107.9°$ and $\delta_z = 2.354$ Å. The crystal-field parameters were taken from complex **A**. The $\Delta\theta$ dependence of the calculated g and $|A|$ components can be compared qualitatively with those obtained by using an angular overlap approach for a penta-coordinate C_{2v} copper(II) complex [18].

The results of the crystal-field calculation for the $d_{xy} > d_{yz,\,xz} > d_{x^2-y^2}$ level scheme are qualitatively consistent with the experimental results in Table 2. The calculation for the C_{2v} distortion shows qualitative accordance with the changes observed in the g_z and $|A_z|$ values increasing and decreasing, respectively, from **C** to **B**.

ESR spectra

The ESR spectra measured in toluene–chloroform glassy solution at 77 K appear in Fig. 5. The anisotropic ESR parameters were estimated with a trial-and-error simulation method. The simulated spectra in Fig. 6 are not exhaustive, because of ignoring the isotope mixture of the copper ion and the higher order corrections. The parameters estimated are summarized in Table 2.

The ESR spectra of **A** and te**A** show the line shape typical of a system with axially symmetric $\boldsymbol{g}$ and $\boldsymbol{A}$ tensors. The fact that $g_\parallel > g_\perp$ reveals that the $3d_{x^2-y^2}$ electronic configuration dominantly contributes to the ground state doublet. In both the $g_\perp$ and $g_\parallel$ regions, **A** exhibited a nine-line superhyperfine structure due to the equivalent four nitrogen nuclei. te**A** also exhibited a similar but less resolved superhyperfine structure in unstable methanol and ethanol glasses. A 30% ethylene glycol aqueous stable glass improved the resolution in the $g_\perp$ region but scarcely so in the $g_\parallel$ region. These ligand hyperfine splittings are ascribed to the C_{4v} symmetry of the effective ligand field in solution.

The g_z values showed the concomitant increasing order of te**A** < **A** < **C** < **B** with decreasing series of $|A_z|$ values of te**A** > **A** > **C** > **B**. This order parallels the tbp% and τ value or the distortion from C_{4v} square pyramidal geometry.

TABLE 2 Spectroscopic data observed for the copper(II) complexes of the chiral cyclens

Complex	AB, CD and MCD transition energy in wave number of d–d* transition region[a]			ESR parameters[b]									
	AB	CD	MCD	g_z	g_x	g_y	A_z	A_x	A_y	a_{Cu}	$A_{\parallel}^{N}$	$A_{\perp}^{N}$	$A_{\parallel}^{Cl}$
teA[c]	15 6	14 3	14.0[d]	2 210		2 052	180		13	68		10 9	
	(256)	17 1	17 2[e]										
A(A_R, A_S)	14.4	13 4	13.4[d]	2 218		2 056	175		13	67	9 2	10 1	
	(570)	16 3	15 6[e]										
C	13.7		12.7[d]	2 223	2 048	2 076	165	24	25	61			
	(570)		15.0[e]										
B	12 9		10.2[f] [10 7][h]	2.230	2.047	2 092	161	14	24	62			
	(545)		14 2[g] [14 2][h]										
D	8.7(221)		8 2[f] [9.1][h]	2 014	2.232	2 139	44	127	64	60			17
	12.0(285)		11 2[g] [10 5][h]	[2.008	2 245	2 156	43	122	71][i]				
			[12 9][h]										

[a]The band position is measured in kcm^{-1} with ϵ value (M^{-1} cm^{-1}) in parentheses [b]The anisotropic parameters were obtained from the glassy solution at 77 K. A^N and A^{Cl} are the nitrogen and chlorine superhyperfine tensor component designated. a_{Cu} is the isotropic hyperfine coupling constant observed at room temperature. Every hyperfine coupling constant is of its absolute value in 10^{-4} cm^{-1} [c]The electronic and ESR spectra of this complex were measured in methanol solution and in ethanol glass, respectively. The electronic and ESR spectra of the other complexes were observed in chloroform and in toluene (5–10%)–chloroform glass, respectively [d]Faraday A term energy [e]B term energy [f,g]The energy at extremum with positive and negative $\Delta\epsilon$, respectively [h]The excitation energy estimated by curve fitting [i]These data were obtained from the single-crystal ESR experiment

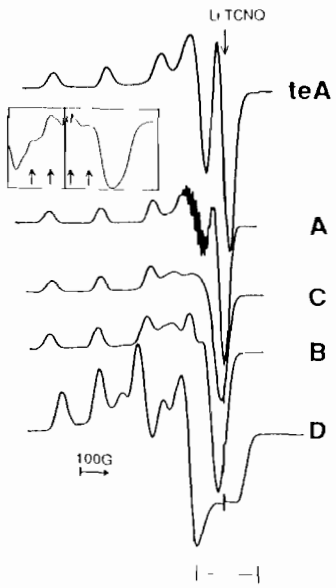

Fig. 5. ESR spectra of copper(II) complexes observed at 77 K. The inset is the second-derivative ESR spectrum of **D** whose abscissa range is shown by a range bar in the first-derivative spectrum. The arrows in the inset indicate the superhyperfine splitting due to the chlorine nucleus and the sharp line originates in Li–TCNQ.

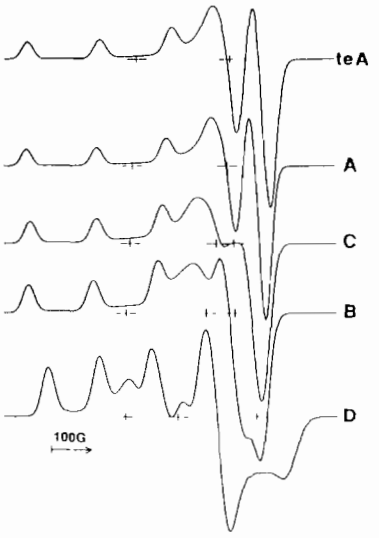

Fig. 6. Simulated ESR line shape due to the g and A anisotropy. The cross marks show the positions of g_z, g_y and g_x components

The lowest g component of **D** is very close to 2.00 but the lowest ones of the others exceed 2.045. This g value of **D** can be attributed to a $3d_{z^2}$ type ground state doublet. The second-derivative ESR spectrum of **D** observed at 77 K revealed four peaks with a separation of 17×10^{-4} cm^{-1}, as shown in an inset in Fig. 5. This is a reasonable value for a parallel superhyperfine splitting due to the chlorine atom ($A_{\parallel}^{Cl}$) on which the spin density of 0.011 will be estimated later. This reveals that the principal z axis of the g tensor lies along the Cu–Cl bond. This also supports our assumption of the compressed square pyramid, because the Cu–Cl axis is the principal axis of the C_{2v} symmetry but never the unique axis perpendicular to the trigonal plane in which the Cu–Cl bond lies (see Fig. 10). For the $[CuN_4S]$ chromophore in the $[Cu(bipy)_2(thiourea)](ClO_4)_2$ crystal, the z axis was found to be perpendicular to the

trigonal plane composed of two nitrogens and one sulfur [10].

The isotropic nitrogen superhyperfine tensor of **A** indicates a more dominant σ- than π-bonding character in the Cu–N bonds [19a] and hence little contribution of the $3d_{xy}$ electronic configuration to the ground state doublet. Actually large isotropic couplings of σ- and π-radicals with considerable s character and anisotropic couplings of π-radicals have been observed [19b]. An example for a very anisotropic ligand hyperfine splitting was observed to be $A_{\perp}^{Cl}=7.8\times10^{-4}$ cm^{-1} and $A_{\parallel}^{Cl}=0$ for $3d_{xy}$ ground state $[CrOCl_5]^{2-}$ [20].

$A_{\parallel}^{N}$ and $A_{\parallel}^{Cl}$ due to dipolar coupling between the electron spin on the copper ion and the nuclear spin in the atom designated are calculated to be below 0.5×10^{-4} cm^{-1} based on the point dipolar approach: $A_{\parallel}^{dipolar}=2g\beta g_N\beta_N r^{-3}$. Therefore, the observed ligand hyperfine couplings can be attributed to covalency. Chlorine hyperfine splitting is observed only for **D**, because its $3d_{z^2}$ ground state orbital is pointing to the Cu–Cl bond but the $d_{x^2-y^2}$ orbitals for the others are not in the direction of that bond.

AB, CD and MCD spectra

The AB and MCD spectra appear in Fig 7. Two or more d–d* transitions of higher intensity may be predicted for a square pyramid [21]. However, the AB spectra of **A**, **C** and **B** show a single band with an unusually large molar extinction coefficient, ϵ (500–600 M^{-1} cm^{-1}). On the other hand, the AB spectrum of **D** exhibits two apparent component absorptions with an ϵ value half that of the above complexes. Comparing the spectra of **A**, **C** and **B** with that of **D**, the former spectra may be composed of the possible d–d* transitions. The bandwidth of te**A** without an N-benzyl group is much greater than those of the others, which may be attributed to the larger fluctuation of the $3d_{x^2-y^2}$ level due to the Cu–N stretching motion. Styka *et al.* [12b] proposed that the increasing ϵ from Cu–cyclen ($\epsilon=200$–300) to Cu–tetrabenzylcyclen (500–900) indicated a greater degree of distortion and consequently greater d–p mixing. However, there does not appear to be such a correlation between the ϵ value and the distortion of the present complexes. The energies of the absorption maxima are presented in Table 2.

The CD curves of $\mathbf{A}_R$ and te$\mathbf{A}_R$ are shown in Fig. 8. Those of $\mathbf{A}_S$ and te$\mathbf{A}_S$ are observed to be strict mirror images of $\mathbf{A}_R$ and te$\mathbf{A}_R$, respectively. The energies at the CD extrema are also listed in Table 2. Metal coordination at the nitrogen atoms generates new chiral centers. The configurations of the asymmetric nitrogens in $\mathbf{A}_R$ and te$\mathbf{A}_R$ have been found to be *RRRR* and *SSSS*, respectively [11a]. The CD curves of $\mathbf{A}_R$ and te$\mathbf{A}_R$ are approximately enantiomeric with each other. This suggests that the sign of CD in the d–d* band region depends on the configuration of the asymmetric nitrogens. In the CD spectra of $\mathbf{A}_R$ and te$\mathbf{A}_R$, the d–d* bands observed as a broad single band in AB split into two component extrema, respectively. The absorption maximum in the AB spectrum of each complex is located at the midpoint of the two CD extrema. Since the $d_{z^2}\leftrightarrow d_{x^2-y^2}$ magnetic dipolar transition is forbidden in C_{4v} symmetry, the two CD bands are assigned to the $d_{xy}\leftrightarrow d_{x^2-y^2}$ and degenerate $d_{yz,xz}\leftrightarrow d_{x^2-y^2}$ excitation.

In order to discriminate between the non-degenerate and degenerate excitations, the energies of these CD extrema have been compared with those of the MCD spectra. The larger CD wave numbers of $\mathbf{A}_R$ and te$\mathbf{A}_R$ agree fairly well with those of the MCD extrema at the high energy side. These MCD extrema can be assigned to the positive *B* term. The low energy CD wave numbers coincide excellently with those at the MCD spectral line crossing over the zero line. This

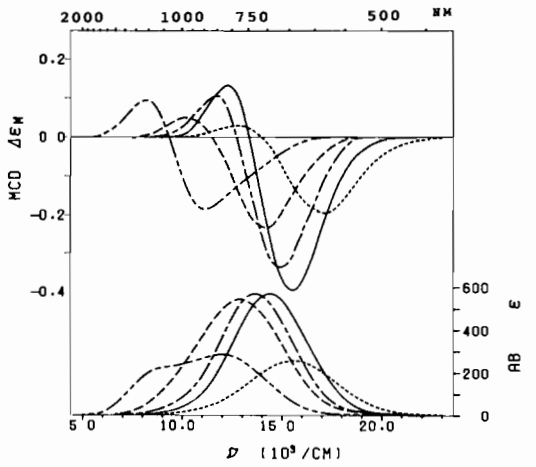

Fig. 7. Optical absorption and magnetic circular dichroism spectra of **A** (——), **B** (– – –), **C** (– – –), **D** (– · – ·) and te**A** (– · – ·) observed in chloroform (**A**, **B**, **C** and **D**) and in methanol (te**A**).

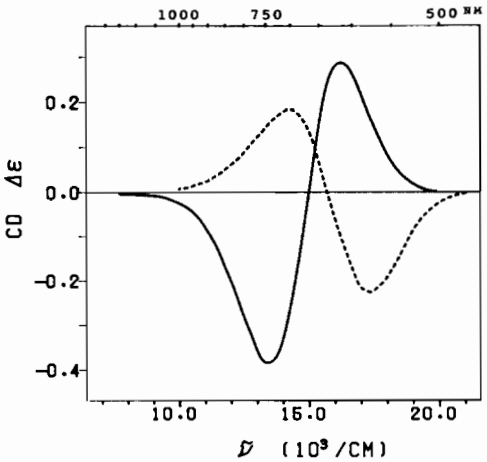

Fig. 8. Circular dichroism spectra of **A** (——) in chloroform and te**A** (– · – ·) in methanol.

crossing over can be attributed to the anomalous A term dispersion. The A term dispersion can be ascribed to the location of a degenerate excitation $d_{yz,xz} \leftrightarrow d_{x^2-y^2}$. Similar dispersions have been observed for several copper(II) complexes of derivatives of 1,4,8,11-tetraazacyclotetradecane (cyclam) [22]. The crystal-field calculation, which necessitates these two energy separations but not the separation between the $d_{x^2-y^2}$ and d_{z^2} levels, predicts the following orbital sequence for the $3d^1$ positive hole; $d_{x^2-y^2} < d_{z^2} < d_{yz,xz} < d_{xy}$. The MCD energies are given in Table 2.

The above MCD assignment is based on the interpretation that the spectrum is a superposition of Faraday A term dispersion and B term extremum. This is an approximation valid in the absence of spin–orbit interaction [23]. In the presence of that coupling, the alternatives to our A term may be superposition of C terms or/and B terms with opposite sign. If it were so, however, the excellent agreement of the CD extremum with the MCD crossing-over point observed for both $\mathbf{A}_R$ and te$\mathbf{A}_R$ could not be explained. It is noted that the spin–orbit coupling constant is about -0.6 kcm^{-1} (will be estimated later) whose magnitude is equal to the first-order perturbed splitting width from the unperturbed system [23] and rather smaller than the bandwidth. Therefore, the difference between the MCD spectral shape with and without the spin–orbit coupling will be small; the above assignment is rationalized.

Since the MCD spectra of C_{2v} or lower symmetry must be composed of more components than those of C_{4v}, the whole spectral shape should be considerably altered by the overlapping, individual intensities, and so on. However, in the absence of temperature-dependent MCD measurements we are unable to discriminate C term from A and B terms. In order to obtain the additional information about the MCD excitations, the following relation was employed [24].

$$x = e/d = \frac{\sqrt{3}a/\Delta E_{z^2,xz} - b/\Delta E_{x^2-y^2,xz}}{\sqrt{3}a/\Delta E_{z^2,yz} + b/\Delta E_{x^2-y^2,yz}} \tag{5}$$

where a, b, d and e are the orbital coefficients of Kramers doublets, discussed later. When the coefficient a is zero (the C_{4v} case), the ratio becomes necessarily -1.00. The ratio is estimated to be -1.043 for **C** from the ESR parameters (see Table 3). In view of this value and the trigonality parameters, the MCD of **C** with the d_{yz} and d_{xz} levels in close proximity may be assigned along the same lines that we adopted for te**A** and **A**.

The above ratio is insensitive to $\Delta E_{x^2-y^2,z^2}$ [24], so we could infer the level scheme based on a $\Delta E_{x^2-y^2,z^2}$ assumed adequately when the other three excitation energies are known. Because the MCD spectrum of **D** showed a small shoulder, spectral decomposition was undertaken using the SP program [25]. Three Gaussian components were obtained as shown in Fig. 9. Taking a partial level scheme such as $\Delta E_{z^2,xz} = 9.1$, $\Delta E_{z^2,yz} = 10.5$ and $\Delta E_{z^2,xy} = 12.9$ kcm^{-1}, the assumed lowest excitation energies of $\Delta E_{z^2,x^2-y^2} = 5.0$ and 3.0 kcm^{-1} for **D** gave the ratios of 0.77 and 0.87, respectively. The former ratio agrees with 0.778 estimated from the ESR parameters. However, a limiting effort for **B** was made in vain, because the ratio is sensitive to the ΔEs that appear explicitly in the above equation. Nevertheless, the maximum energy d–d* bands of the present complexes are ranged between 17 and 13 kcm^{-1}. On the other hand, Hathaway reported that the maximum d–d* bands of square pyramidal $Cu(NH_3)_5X_2$ and $Cu(NH_3)_4X_2$ complexes are distributed in a very narrow range 15.8–16.3 kcm^{-1} [14]. Therefore, the present maximum d–d* bands are sufficiently lower than those, which is attributed to the in-plane loose coordination due to the distortion around the copper ion.

Relation between ESR parameters and stereochemistry

The d_{z^2} and $d_{x^2-y^2}$ orbitals belonging to A_1 and B_1 in C_{4v} symmetry are in the same A_1 representation in C_{2v}. Accordingly, the proper ground state doublet for the present case must contain a linear combination of the two orbitals. A similar but more general case was treated by Swalen *et al.* [15]; their Kramers doublets for $3d_{x^2-y^2}$ and $3d_{z^2}$ type ground states are:

$$\Psi^\alpha = a|z^{2\alpha}\rangle + b|x^2-y^{2\alpha}\rangle + c|xy^\alpha\rangle - id|yz^\beta\rangle - e|xz^\beta\rangle \tag{6a}$$

$$\Psi^\beta = i(a|z^{2\beta}\rangle + b|x^2-y^{2\beta}\rangle - ic|xy^\beta\rangle - id|yz^\alpha\rangle - e|xz^\alpha\rangle) \tag{6b}$$

where superscripts α and β designate the spin functions. The orbital coefficients a, b, $\cdots$ are all real quantities. The expressions for the g components are.

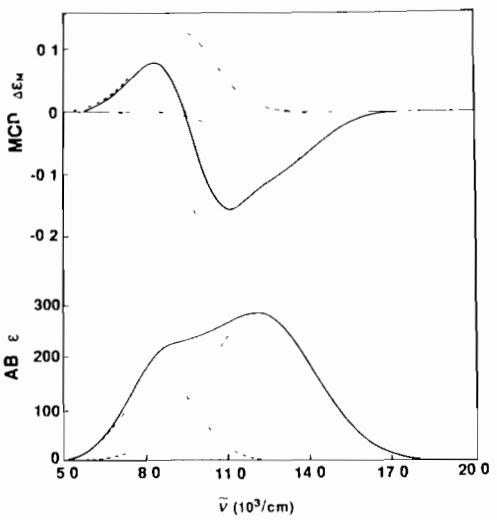

Fig 9 Observed (——) and Gaussian components (- - - -) of the magnetic circular dichroism spectrum (top) and optical absorption (bottom) of **D**

$$g_z = 2 - 4d^2 - 4e^2 + 8bc + 4de \quad (7a)$$

$$g_x = 2 - 4c^2 - 4e^2 + 4\sqrt{3}ad - 4ce + 4bd \quad (7b)$$

$$g_y = 2 - 4c^2 - 4d^2 + 4\sqrt{3}ae - 4be + 4cd \quad (7c)$$

Along with the normalization condition, the non-linear simultaneous eqns. (7) are solved for five unknowns a, b, c, d and e in the first place. The validity of the numerical solution is checked with the observed copper hyperfine tensor. In the course of the check, two unknowns P and κ are estimated with a least-squares fit to the hyperfine components.

$$\begin{aligned} A_z = P[&8bc + 4de + (6\xi - \kappa)(1 - 2d^2 - 2e^2) \\ &- 3\xi\{4c^2 + 4b^2 - d^2 - e^2 + \sqrt{3}a(d + e) \\ &+ 3(d - e)(c - b)\}] \end{aligned} \quad (8a)$$

$$\begin{aligned} A_x = P[&4\sqrt{3}ad - 4ce + 4bd + (6\xi - \kappa)(1 - 2c^2 - 2e^2) \\ &- 3\xi\{(\sqrt{3}a + b)^2 - c^2 + 4d^2 - e^2 - \sqrt{3}a(e + 2c) \\ &+ 3cd - 3be + 3de\}] \end{aligned} \quad (8b)$$

$$\begin{aligned} A_y = P[&4\sqrt{3}ae + 4dc - 4be + (6\xi - \kappa)(1 - 2c^2 - 2d^2) \\ &- 3\xi\{(\sqrt{3}a - b)^2 - c^2 - d^2 + 4e^2 - \sqrt{3}a(d - 2c) \\ &- 3ce + 3bd + 3de\}] \end{aligned} \quad (8c)$$

where ξ is related to the electronic configuration of the ion:

$$\xi = [(2l+1) - 4S]/[S(2l-1)(2l+3)(2L-1)] \quad (9)$$

and the present case of $l = L = 2$ and $S = 1/2$ hence gives $\xi = 2/21$ [17].

The above procedure was carried out on a VAX station 3200*. For the best 50 solutions in the residual sum of squares for the least-squares refinement, the residual sums were plotted against the $x(=e/d)$ value. The graph showed one, two or three minimal sums; the P and κ parameters that gave the minima are shown in Table 3. The sums for the possibles ranged from 3×10^{-2} to 5×10^{-11} in $(10^{-4}\ \mathrm{cm}^{-1})^2$ through all the complexes. The following criteria were employed to select the most reasonable solution among the possibles. (i) The observed isotropic copper hyperfine coupling constant must compare with the calculated one. (ii) The P and κ parameters must be less than those of the free ion, $P_0 = 360\times10^{-4}\ \mathrm{cm}^{-1}$ and $\kappa_0 = 0.43$ [26], taking account of the covalency. (iii) The parameters must be consistent with the results of the electronic spectral and crystallographic studies. A tolerable difference was obtained between the observed and calculated isotropic hyperfine coupling constants. The P, κ and $P\kappa$ parameters for **A** are fairly consistent with those estimated by the following method. The electron–nuclear dipolar term, P (see eqn. (12)), and the factor to give Fermi contact term, κ, were estimated to be $P = 274\times10^{-4}\ \mathrm{cm}^{-1}$ and $\kappa = 0.327$, providing $P = \rho P_0$ [27] and $\kappa = \rho\kappa_0$ [26]. The net spin density on the 3d orbitals was estimated to be $\rho = 0.76$ with the nitrogen superhyperfine splitting [28]. The spin–orbit coupling constant of $-630\ \mathrm{cm}^{-1}$ was also evaluated with $\lambda = \rho\lambda_0$ [27] and $\lambda_0 = -828\ \mathrm{cm}^{-1}$ [26]. The same consistency can be concluded for te**A**, since a similar superhyperfine coupling constant to that of **A** was observed. Similar calculation gave a spin density of 0.011 on the chloride ion of **D**. The propriety of the solution can also be checked by the following approximate relation valid for the case of parallel and perpendicular A components possessing the same sign [29]:

$$P\kappa = |a_{\mathrm{Cu}}| + P\Delta g_{\mathrm{av}} \quad (10)$$

where a_{Cu} and Δg_{av} are the observed isotropic hyperfine coupling constant and the difference between the average of the observed g components and g_e, respectively. The κ values estimated from this relation are 0.374 and 0.381 for te**A** and **A**, respectively; the consistency is encouraging. Therefore, we may reach conclusions by using the above parameters and the orbital coefficients. Note that the sign of a depends on the sign (or the definition) and magnitude of the anisotropy.

$$a = \frac{(g_x - g_y) + 4(x^2 - 1)d^2 + 4(1 + x)(c - b)d}{4\sqrt{3}(1 - x)d} \quad (11)$$

where x is $-1.5 \sim -0.5$ for the $d_{x^2-y^2}$ and $0.5 \sim 1.5$ for the d_{z^2} type ground state doublet.

The signs of the A tensor components are assigned as in Table 3. The negative values of all the calculated isotropic hyperfine coupling constants are consistent with the exchange polarization mechanism for the inner s-spin (ref. 30a and refs. therein). The observed isotropic hyperfine coupling constants are in decreasing order from te**A** to **D**. P and κ are also in a similar descending order, except for **C**. The decreasing P parameters suggest that the 3d orbitals expand slightly ($\sim 10\%$) owing to the covalency. The κ parameter which was introduced as a numerical factor for the admixture of configurations with unpaired s electrons [17] may be correlated with the exchange polarization of the inner s-spin. The slight expansion of the inner s orbitals associated with the 3d orbital expansion reduces the s-spin density at the

*FORTRAN program was coded. The iteration at given $x_0 = e/d$ was continued till the variation in the residual sum of squares became to be smaller than 10^{-16}, the fittings of P and κ for the eight possibilities in the signs of As were done to the optimal shifts that were smaller than 10^{-8} times the corresponding parameters. The seven parameters at $x_1 = x_0 + 0.001$ were obtained using the a_0, b_0, c_0 and d_0 as the starting parameters of the iteration. The best 50 solutions in the residual sum of squares for the least-squares refinement were collected.

TABLE 3. The g components used in Swalen's calculation [15], orbital coefficients of Kramers doublet, and calculated parameters[a]

Complex	g_z	g_x	g_y	a	b	c	d	$x=e/d$	A_z	A_x	A_y	P	κ	$P\kappa$	a_{Cu}[b]	A_{iso}[c]
teA	2 210	2 052		0 0000	0 9996	0 0265	0.0135	−1.000	−180	−13	−13	250	0 381	95.5	68	−68 7
				0 0000[d]	*0 9996*	*0 0265*	*0 0135*	*−1 000*	*−180*	*13*	*13*	*290*	*0 284*	*82 3*		*−51 3*
A	2 218	2 056		0 0000	0 9995	0 0276	0.0146	−1 000	−175	−13	−13	245	0 386	94.7	67	−67 0
				0 0000	*0 9995*	*0 0276*	*0 0146*	*−1 000*	*−175*	*13*	*13*	*285*	*0 287*	*81 8*		*−49 6*
C	2 223	2 048	2.076	−0.1130	0 9931	0 0285	0 0158	−1 043	−165	24	−25	259	0 333	86.1	61	−54.7
				−0 0190	*0 9993*	*0 0283*	*0 0131*	*−1 454*	*−165*	*−24*	*−25*	*214*	*0 453*	*96 8*		*−71 3*
				−0 0148	*0 9994*	*0 0283*	*0 0130*	*−1 475*	*−165*	*24*	*25*	*288*	*0 253*	*72 9*		*−38 7*
B	2 230	2.047	2.092	−0 1053	0 9939	0 0294	0 0153	−1 313	−161	14	−24	246	0 359	88.1	62	−57.0
D[e]	2 008	2.245	2.156	0.9854	0 1647	0 0089	0 0333	0 778	43	−122	−71	241	0 349	83.9	60	−50 0
				0 9534	*0 2986*	*0 0049*	*0 0320*	*0 923*	*−43*	*−122*	*−71*	*113*	*0 839*	*94.7*		*−78 7*
D[f]	2 014	2.232	2.139	0 9797	0.1964	0.0109	0 0311	0 760	44	−127	−64	239	0 338	80.6	60	−49 0

[a]The common unit of A_i, P and $P\kappa$ is 10^{-4} cm^{-1}. [b]Isotropic copper hyperfine coupling constant observed at room temperature [c]The same constant based on the calculated A_z, A_x and A_y. [d]The data written in italics result in improper solutions, the reason is given in the text. [e,f]The g and A tensors used in the calculation are of single crystal and glassy solution, respectively

nucleus and hence decreases the Fermi contact term interaction. Therefore, a consistent trend is also found between $P\kappa$ and a_{Cu}. However, the reason for the irregular magnitudes of P and κ for **C** has not yet been realized.

The remarkable result for te**A**, **A**, **C** and **B** is that $c<2d$ and $c<2|e|$. The partial orbital sequence of $d_{xy} > d_{yz,xz}$ discussed previously is consistent with this relation, taking account of eqns. (3). The above relation results from the smallness of the c coefficients; actually typical c values are around 0.04 [31]. The in-plane antibonding $d_{x^2-y^2}$ orbital (in terms of MO scheme) must be more sensitive to the distortion around the square pyramidal copper ion than the non-bonding d_{xy} orbital. Therefore, the copper displacement from the N-basal plane raises the $d_{x^2-y^2}$ level for the hole, which is illustrated in Fig. 4. Inevitably the basal Cu–N bonds are elongated, which is followed by the reduction of the apical Cu–Cl bond length.

The half-filled 3d orbital of **D** is unequivocally d_{z^2}. The positive sign and small magnitude of A_z are reasonable for the d_{z^2} half-filled configuration [32]. The magnitude is however smaller than those described as expectable in ref. 32b. The electron–nuclear dipolar coupling in the same atom is given by:

$$A_{aniso} = \frac{g\beta_e g_N \beta_N}{\langle r^3 \rangle} \frac{\langle 3\cos^2\alpha - 1\rangle}{2} (3\cos^2\theta - 1)$$

$$= \frac{\langle 3\cos^2\alpha - 1\rangle}{2} P(3\cos^2\theta - 1) \qquad (12)$$

where the symbols are the same as those used in ref. 30a. The value of $C = \langle 3\cos^2\alpha - 1\rangle$ is dependent on the half-filled orbital.

$C = +4/7$ for d_{z^2} half-filling (13a)

$C = +2/7$ for $d_{yz,xz}$ half-filling (13b)

$C = -4/7$ for $d_{x^2-y^2,xy}$ half-filling (13c)

Consequently, the d_{z^2} ground state tensor is $(A_{zz}, A_{xx}, A_{yy}) = (4P/7, -2P/7, -2P/7)$ and the $d_{x^2-y^2}$ ground state tensor is $(-4P/7, 2P/7, 2P/7)$ which is the case of te**A** and **A** ($A_x = A_y = +13$ for $a_{Cu} = 68$ in 10^{-4} cm^{-1} is contradictory to this, ignoring the smaller contribution from the g anisotropy [30b]) Therefore, the small positive A_z of **D** results from the negative A_{iso} (-50×10^{-4} cm^{-1}) and the positive A_{zz} (93×10^{-4} cm^{-1}) whose magnitudes seem to be closer to each other than those in usual cases.

It is noticeable that the c of **D** is very small, compared with b which is very large in contrast. These two coefficients should be equal to each other for the regular trigonal bipyramid; the examples are $Ag[Cu(NH_3)_2(SCN)_3]$ with $b=c=0.0313$ and slightly distorted $[Cu(bipy)_2I]I$ with $b=0\,0661$ and $c=0.0671$ [10]. Small $c=0.017$ and large $b=0.159$ for $[Cu(bipy)_2(thiourea)](ClO_4)_2$ have been attributed to a distorted trigonal bipyramid [10]. The surprisingly small c of **D** implies the highest $3d_{xy}$ level which has been adopted for the examination of the MCD spectrum of **D**.

Using the correlation diagram for Berry pseudorotation [8a], the orbital coefficients are rearranged in Table 4. The coefficients in the 5th column decrease from 0.9996 to 0.9854, which shows that the Cu–N bonds are destabilized with the increasing distortion. The ascending order in the magnitudes of the coefficients in the 4th, 7th and 8th columns indicates the reduction of the Cu–Cl bond distance (see Table 1).

The apparent trigonal bipyramidal character of **D** with $\tau=0.670$ ($\tau=1.0$ for trigonal bipyramid) is as follows (see Fig. 10): the trigonal axial and trigonal equatorial N–Cu–N bond angles are 164.4 and 124.2°, respectively, and the copper displacement from the pseudo-trigonal plane is 0.012 Å [11b]. Although the latter angle is of a trigonal bipyramid, the former is of a square pyramid.

TABLE 4. Variation of the orbital coefficients of Kramers doublet with the angular-structure parameters[a]

Complex	τ	tbp%	d_{z^2}	$d_{x^2-y^2}$	d_{xy}	d_{yz}	d_{xz}
teA	0.010	0	0 0000	0.9996	0 0265	0 0135	−0 0135
A	0.027	0	0 0000	0.9995	0.0276	0 0146	−0 0146
C	0 095	20	−0 1130	0.9931	0.0285	0 0158	−0 0165
B	0.328	30	−0 1053	0.9939	0.0294	0 0153	−0 0201
D	0.670	70	0 1647	0.9854	0.0089	0 0333	0.0259
			$d_{x^2-y^2}$	d_{z^2}	d_{xy}	d_{yz}	d_{xz}

[a]The 3d orbitals for the given coefficients of teA, A, C and B are designated in the top row and those of D are in the bottom row. The definition of the parameters of τ and tbp% are given in refs. 5b and a, respectively.

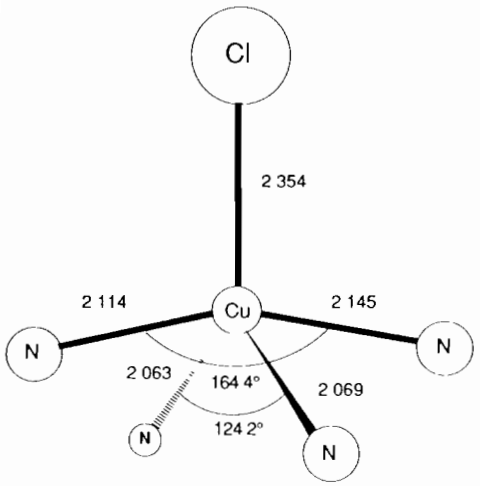

Fig. 10 Stereochemistry of $[CuN_4Cl]$ chromophore of **D**. The bond lengths are in Å.

Further, the axial bond length (av. 2.130 Å) is significantly longer than the equatorial one (2 066 Å), which is the reverse of a normal trigonal bipyramidal copper(II) complex but is as in a square pyramid [9, 33]. A similar reversal can be found for **B**. Since the 3d positive hole of the copper(II) ion exclusively populates the $3d_{x^2-y^2}$ or $3d_{z^2}$ orbital, its strongest interaction with the negative charge of the ligand must be via pointing at the lobes of the half-filled orbital. From this point of view, the principal lobe of the $3d_{z^2}$ orbital of **D** is pointing at the Cu–Cl bond, because this bond is most reduced in length among all of the complexes. This direction is consistent with that determined by the chlorine superhyperfine splitting in the g_z region, so that the geometry in the crystal of **D** remains unchanged in solution. The orbital coefficients of **D** in the doped crystal and in the glassy solution are very similar to each other, as shown in Table 3, also implying a rigid geometry for **D**.

The axially compressed square pyramidal type stereochemistry of **D** accounts for the $3d_{xy}$ level being highest. Bending down of two *trans*-nitrogen atoms in the N-basal plane (by ~20°) and the resulting elongation of the Cu–N bonds reduce the repulsion between the apical chloride ion and the amine groups. Accordingly, the $d_{x^2-y^2}$ level is destabilized and the chloride ion is able to approach the copper ion along the z direction. Leaving the highest d_{xy} level almost unchanged, the d_{z^2} level is stabilized below the $d_{x^2-y^2}$ level. Therefore, the ground state of **D** lacks d_{xy} character.

DeSimone *et al* [12a] reported that unusual kinetic stability of [CuCl(1,4,7,10-tetrabenzylcyclen)]NO_3 might be due to the pyramidal geometry and the difficulty in dissociating the apical chloride. This argument is supported by the present study. All the data of the present complexes can be explained on the basis of the rigid molecular structure and the square pyramidal type geometry compressed along the Cu–Cl bond. This indicates the prohibited re-orientation of the chelating ligand and dissociation of the chloride, so that the present complexes should also be inert in spite of the loose Cu–N bonds.

It is interesting to examine the correlation between the electronic-spectral and ESR parameters, because the stereochemistry and d–d* transition of the complexes in solution are established. The observed $|A_z|$ and g_z values have been plotted against the highest d–d* transition energy, as shown in Fig. 11. Putting eqns. (3) into eqns. (2) and (8a), and neglecting the quadratic terms, the following equations are obtained:

$$g_z = 2[1 - 4\lambda/\Delta E_{x^2-y^2,\,xy}] \quad (14)$$

$$A_z = P[-\kappa - 4/7 - (62/7)\lambda/\Delta E_{x^2-y^2,\,xy}] \quad (15)$$

Providing κ is positive and λ is negative, g_z and $|A_z|$ are monotonous decreasing and increasing functions of the $d_{xy} \leftrightarrow d_{x^2-y^2}$ transition energy, respectively. In fact, the experimental curves in Fig. 11 are monotonic. Accordingly the simple relation of a well-known type between g_z and $|A_z|$ is also expected. In the same Figure, data for the molecular g_z values and the highest d–d* transition energies observed from polarized single-crystal optical spectra of some square pyramidal and square coplanar $[CuN_4X]$ chromophores are given. These data are located on the same curve through the data of the present complexes and of Cu–cyclam with square copla-

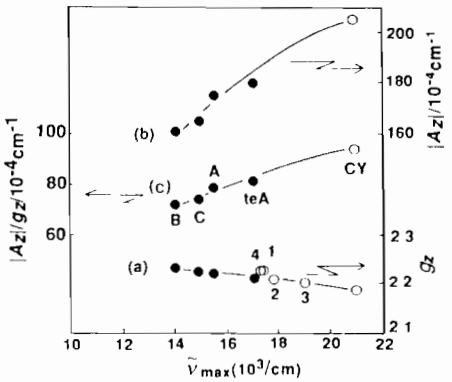

Fig 11. Plots of the observed g_z (a), $|A_z|$ (b) and $|A_z|/g_z$ ratio (c) against the maximum d–d* excitation energy. The symbol CY stands for Cu–cyclam [34] The numbers 1, 2, 3 and 4 represent the data of typical square planar $[Cu(H_2O)(NH_3)_4]SO_4$ [13b, 35] and $[Cu(H_2O)(1,3\text{-pn})_2]SO_4$, and those of square coplanar $Na_4[Cu(NH_3)_4](Cu(S_2O_3)_2)_2\ H_2O$ and $Na_4[Cu(NH_3)_3](Cu(S_2O_3)_2)_2 \cdot H_2O\ NH_3$ [13b], respectively.

nar coordination geometry [34].* The data of **B** may be almost the low energy extreme in this type of graph for the $d_{x^2-y^2}$ ground state $[CuN_4X]$ copper(II) chromophores.

Acknowledgements

We are grateful to Professors H. Kobayashi of Kitasato University, Y. Kaizu of Tokyo Institute of Technology, and Dr K. Yamamoto of RIKEN for valuable discussions. We also thank the referees for some comments and kind correction for the syntax of the manuscript toward traditional Western usage.

References

1 (a) S Tsuboyama, K Tsuboyama, I Higashi and M. Yanagita, *Tetrahedron Lett*, (1970) 1367, (b) K. Tsuboyama, S Tsuboyama, J. Uzawa and I. Higashi, *Chem Lett*, (1974) 1367

2 (a) T. Sakurai, K Kobayashi, K Tsuboyama and S. Tsuboyama, *Acta Crystallogr, Sect B, 34* (1978) 3465, (b) H Hiramatsu, T Sakurai, K Tsuboyama and S Tsuboyama, *Acta Crystallogr, Sect B, 35* (1979) 1241; (c) T Sakurai, H Hiramatsu, K Tsuboyama and S Tsuboyama, *Acta Crystallogr, Sect B, 36* (1980) 2453; (d) T Sakurai, Y Watanabe, K Tsuboyama and S Tsuboyama, *Acta Crystallogr, Sect B, 37* (1981) 613; (e) T. Sakurai, K Kobayashi, T. Kanari, I Kawata, S. Tsuboyama and K Tsuboyama, *Acta Crystallogr, Sect B, 39* (1983) 84

3 K Tsuboyama, S Tsuboyama, J Uzawa and T Sakurai, *Tetrahedron Lett*, (1977) 4603

4 T Sakurai, K. Kobayashi, K Tsuboyama and S Tsuboyama, *Acta Crystallogr, Sect B, 34* (1978) 1144

5 (a) R.R. Holmes and J A Deiters, *J Am Chem Soc, 99* (1977) 3318, (b) A W. Addison, T N Rao, J Reedijk, J van Rijn and G C Verschoor, *J Chem Soc, Dalton Trans*, (1984) 1349.

6 T Sakurai, K. Tsuboyama, S Tsuboyama and K Kobayashi, *J Cryst Soc Jpn, 25* (1983) 299

7 R.S Berry, *J Chem Phys, 32* (1960) 933; *Rev Mod Phys, 32* (1960) 447

8 (a) A R Rossi and R Hoffmann, *Inorg Chem, 14* (1975) 365, (b) P. Meakin, E L. Muetterties and J P Jesson, *J Am Chem Soc, 94* (1972) 5271, (c) R B King, *Coord Chem Rev, 122* (1993) 91.

9 N J Ray. L Hulett, R. Sheahan and J Hathaway, *J Chem Soc, Dalton Trans*, (1981) 1463.

10 K T McGregor and W E Hatfield, *J Chem Soc, Dalton Trans*, (1974) 2448.

11 (a) T Sakurai, K Kobayashi, A Hasegawa, S. Tsuboyama and K. Tsuboyama, *Acta Crystallogr, Sect B, 38* (1982) 107, (b) K Kobayashi, T. Sakurai, A Hasegawa, S. Tsuboyama and K. Tsuboyama, *Acta Crystallogr, Sect B, 38* (1982) 1154, (c) T Sakurai, K Kobayashi, H Masuda, S Tsuboyama and K. Tsuboyama, *Acta Crystallogr, Sect C, 39* (1983) 334, (d) S Tsuboyama, K Kobayashi, T Sakurai and K Tsuboyama, *Acta Crystallogr, Sect C, 40* (1984) 1178

12 (a) R.E DeSimone, E L Blinn, K F Mucker, *Inorg Nucl Chem Lett, 16* (1980) 23, (b) M C Styka, R C. Smierciak, E L Blinn, R E DeSimone and J V. Passariello, *Inorg Chem, 17* (1978) 82.

13 (a) B.J. Hathaway and P G Hodgson, *J Inorg Nucl Chem, 35* (1973) 4071, (b) B J Hathaway and D.E Billing, *Coord Chem Rev, 5* (1970) 143.

14 B J. Hathaway, *Struct. Bonding (Berlin), 14* (1973) 49

15 J D. Swalen, B Johnson and H M Gladney, *J Chem Phys, 52* (1970) 4078

16 (a) Y Li, K. Tajima, K Ishizu and N Azuma, *Bull Chem Soc Jpn, 61* (1988) 4067, (b) Y Kajikawa, T Sakurai, N. Azuma, S Kohno, S Tsuboyama, K Kobayashi, K Mukai and K. Ishizu, *Bull Chem Soc Jpn, 57* (1984) 1454

17 A Abragam and M H L Pryce, *Proc R Soc London, Ser A, 205* (1951) 135

18 (a) C Benelli and D Gatteschi, *Coord Chem Rev, 120* (1992) 137, (b) A Bencini, I Bertini, D Gatteschi and A. Scozzafava, *Inorg Chem, 17* (1978) 3194

19 (a) D. Kivelson and S -K. Lee, *J Chem Phys, 41* (1964) 1896, (b) J E Wertz and J.R Bolton, *Electron Spin Resonance*, McGraw-Hill, New York, 1972, pp 174–178

20 H. Kon and N.E. Sharpless, *J Chem Phys, 43* (1965) 1081.

21 (a) A.A G. Tomlinson and B J Hathaway, *J Chem Soc A*, (1968) 1905, (b) Y. Sugiura, K Ishizu and K Miyoshi, *J Antibiotics, 32* (1979) 453

22 H Kobayashi and B Korybut-Daszkiewicz, *Bull Chem Soc Jpn, 45* (1972) 2485

23 H Katô, *Mol Phys, 24* (1972) 81.

24 R Hirosawa and H. Kon, *J Chem Phys, 56* (1972) 4467.

25 (a) H Miyata and S. Tokuda, *Shokubai (Catalyst), 30* (1988) 311, (b) H. Miyata, K. Fujii, S Inui and Y. Kubokawa, *Appl Spectrosc., 40* (1986) 1177, (c) H. Miyata, *Chem Express, 2* (1987) 643

26 D. Kivelson and R. Neiman, *J Chem Phys, 35* (1961) 149

27 Z Šroubek and K Ždánský, *J Chem Phys, 44* (1966) 3078.

28 (a) K. Ishizu, T Haruta, Y Kohno, K Mukai, K Miyoshi and Y Sugiura, *Bull Chem Soc Jpn, 53* (1980) 3513; (b)

*The evidences for square planar Cu–cyclam in aqueous solution are as follows: (i) axial ESR parameters and equivalency of four N atoms inferred from N superhyperfine structure [34], (ii) the similarity in the AB and MCD spectra with those of copper(II) complexes of two isomeric C,C'-dimethyl derivatives of cyclam [22] In this literature, the degenerate $d_{yz,xz} \leftrightarrow d_{x^2-y^2}$ excitations in the two isomeric derivatives have been clearly evidenced.

J.E. Wertz and J.R. Bolton, *Electron Spin Resonance,* McGraw-Hill, New York, 1972, p 500, Table C

29 K.-E. Falk, E. Ivanova, B. Roos and T. Vanngard, *Inorg. Chem., 9* (1970) 556.

30 (a) B.A. Goodman and J.B. Raynor, *Adv. Inorg. Chem. Radiochem., 13* (1970) 135, 735, and refs. therein, (b) B.R. McGravey, *Transition Met. Chem., 3* (1966) 89

31 J. Pradilla-Sorzano and J.P. Fackler, Jr., *Inorg. Chem., 13* (1974) 38.

32 (a) B. Bleaney, K.D. Bower and M.H.L. Pryce, *Proc. R. Soc. London, 228* (1955) 147; B.B. Wayland, J.V. Minkiewicz and M.E. Abd-Elmageed, *J. Am. Chem. Soc., 96* (1974) 2795, (b) A. Bencini, I. Bertini, D. Gatteschi and A. Scozzafava, *Inorg. Chem., 17* (1978) 3194

33 G. Kodama and H. Nakazawa, *Mukikagaku,* Tokyo-kagaku-dohjin, Tokyo, Japan, 1984, translation of J.E. Huheey, *Inorganic Chemistry – Principles of Structure and Reactivity,* Harper and Row, New York, 3rd edn., 1983

34 K. Miyoshi, H. Tanaka, E. Kimura, S. Tsuboyama, S. Murata, H. Shimizu and K. Ishizu, *Inorg. Chim. Acta, 78* (1983) 23

35 (a) E.H. Carlson and R.D. Spence, *J. Chem. Phys., 24* (1956) 471; (b) H. Abe and K. Ôno, *J. Phys. Soc. Jpn., 11* (1956) 947.